Tidal current observations through Admiralty Inlet from ferry-mounted current profilers

Maricarmen Guerra, Jim Thomson, Tim Prusa, Carol Falkenhayn Maloy, Christopher Krembs & Brandon Sackmann

Journal of Ocean Engineering and Marine Energy

ISSN 2198-6444

J. Ocean Eng. Mar. Energy
DOI 10.1007/s40722-019-00135-w

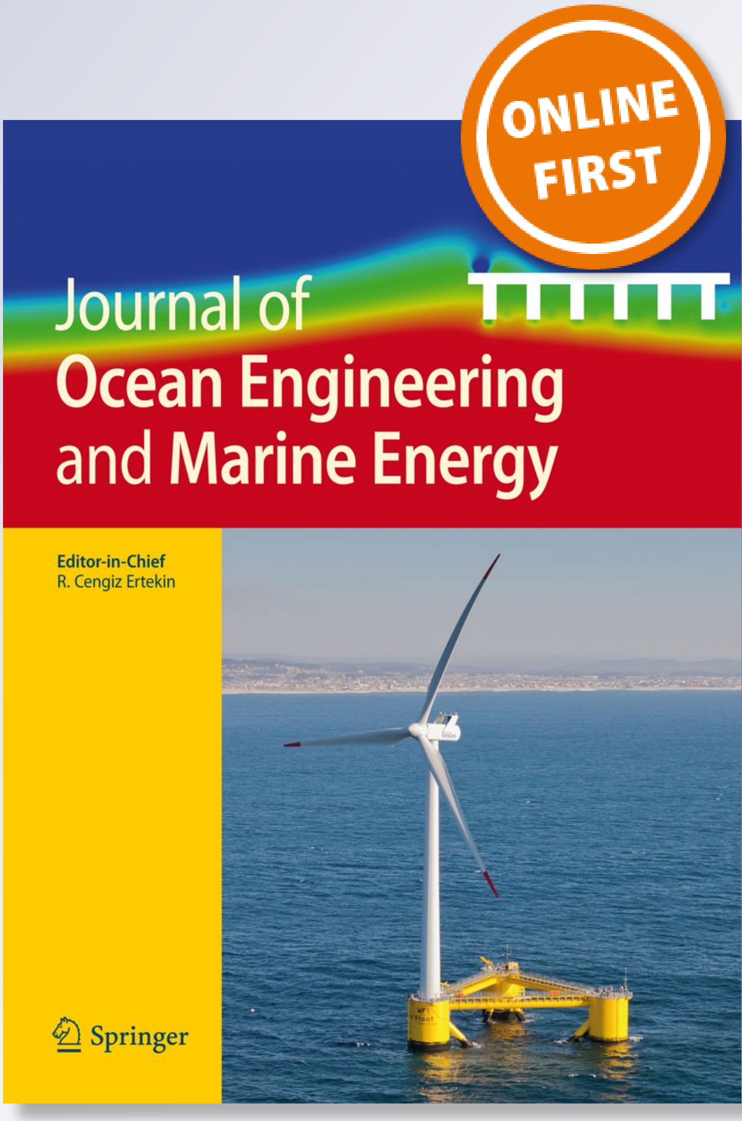

Journal of Ocean Engineering and Marine Energy
https://doi.org/10.1007/s40722-019-00135-w

RESEARCH ARTICLE

Tidal current observations through Admiralty Inlet from ferry-mounted current profilers

Maricarmen Guerra[1,5] · Jim Thomson[1] · Tim Prusa[2] · Carol Falkenhayn Maloy[3] · Christopher Krembs[3] · Brandon Sackmann[4]

Received: 19 October 2018 / Accepted: 17 May 2019

Abstract

Admiralty Inlet is a narrow sill located at the northern end of Puget Sound (WA, USA). Circulation through Admiralty Inlet is complex, with tidal currents exceeding 3 ms^{-1}, large variations in fresh water input to the system, and seasonal ocean water intrusions. Long-term observations of the currents across the entire inlet are crucial for understanding circulation through Puget Sound. In this context, the Washington State Department of Transportation (WSDOT) Ferries, which run year round through Admiralty Inlet, provide a cost-effective platform to mount instruments and obtain long time series of currents distributed across the inlet. Through the Ferry-Base Monitoring of Puget Sound Currents project, two down-looking acoustic Doppler current profilers (ADCPs) are installed on board two WSDOT ferries, providing depth profiles of velocities across the inlet since May 2014. All data are quality controlled and organized in an horizontal and vertical grid across the inlet. Data within each grid cell are analyzed to capture tidal current harmonic components. Results agree well with data from fixed bottom-mounted ADCPs, and show large spatial variability in the amplitude of harmonic components, probably related to the bathymetric features of the inlet. Further analysis provides estimates of tidal asymmetry and residual currents through the inlet, which are relevant to water quality within the Puget Sound.

Keywords Vessel mounted ADCP · Tidal currents · Residual currents · Ferry-based measurements · Tidal energy

1 Introduction

1.1 Ferry-based observations

Previous research projects have demonstrated the utility of ferry-based measurements in the collection of oceanographic data (Merckelbach 2006; Codiga and Aurin 2007; Balfour et al. 2012; Petersen 2014; Nauw et al. 2014; Zhu et al. 2017; Liu et al. 2017). The FerryBox systems have been widely used in ferry lines and commercial vessels in Europe since 2003 (Petersen 2014). These automated systems measure a range of oceanographic parameters, such as temperature, salinity, turbidity, and chlorophyll-*a*. Some FerryBox systems are integrated with acoustic Doppler current profilers (ADCPs) to measure flow velocities, and with a variety of sensors for measuring pH, dissolved oxygen, and nutrients (Petersen 2014). Data from the FerryBox systems have a broad range of applications: from the study of algal blooms to

✉ Maricarmen Guerra
mguerrap@uw.edu

Jim Thomson
jthomson@apl.washington.edu

Tim Prusa
tprusa20@uw.edu

Carol Falkenhayn Maloy
carol.maloy@ecy.wa.gov

Christopher Krembs
ckre461@ecy.wa.gov

Brandon Sackmann
bsackmann@integral-corp.com

1 Applied Physics Laboratory, University of Washington, 1013 NE 40th St, Seattle 98105, WA, USA

2 Civil and Environmental Engineering, University of Washington, 201 More Hall, Seattle 98195, WA, USA

3 Washington State Department of Ecology, 300 Desmond Drive SE, Lacey 98503, WA, USA

4 Integral Consulting Inc., 1205 West Bay Road NW, Olympia 98502, WA, USA

5 Present Address: Oceanography Department, Dalhousie University, 1355 Oxford St, Halifax, NS B3H 4R2, Canada

Published online: 10 June 2019

the validation of remote-sensing measurements of ocean surface properties (Petersen 2014). Recently, acoustic Doppler current profilers have been mounted on board ferry systems covering long transects [$\mathcal{O}(1000)$ km], measuring flow velocities through the water column. Continuous ferry-based measurements along the eastern edge of the East China Sea provided up to eight tidal harmonic constituents in Liu et al. (2017), and data from the same ferry system were successfully used to estimate residual currents from the north-west Pacific Ocean into the East China Sea in Zhu et al. (2017). Acoustic backscatter data from ferry-mounted ADCPs have been used to estimate average suspended sediment concentrations through the Marsdiep inlet ($\sim$ 3 km wide) in The Netherlands in Merckelbach (2006) and Nauw et al. (2014).

1.2 Site description

Puget Sound is a estuarine system located in the north-west of the USA (47.85°N–122.43°W). The main connection between Puget Sound and the Strait of Juan de Fuca (thus the Pacific Ocean) is through Admiralty Inlet, a narrow sill located in the northern part of Puget Sound (48.14°N–122.71°W) (Sutherland et al. 2011).

Admiralty Inlet is a highly energetic constriction, where fast tidal currents are observed and strong tidal mixing occurs. Previous measurements of tidal currents and turbulence at Admiralty Inlet, from fixed bottom-mounted instruments, indicate that maximum velocities are above 3 ms^{-1} mid-channel and faster flows occur near Admiralty Head (north–east), where turbulence intensity is about 10% (Polagye and Thomson 2013; Thomson et al. 2012). Estuarine circulation patterns have been observed at different locations across Admiralty Inlet from long-term fixed bottom-mounted measurements of velocities, with maximum residual velocities reaching up to 0.4 ms^{-1} and strong tidal asymmetries (Deppe et al. 2018; Polagye and Thomson 2013). Seasonal variations of these residual currents are mainly related to freshwater inputs and tidal phase (Deppe et al. 2018), and are associated with low-oxygen ocean water intrusions into Puget Sound, impacting water-quality and marine life through the estuary. Deppe et al. (2018) showed that these low-oxygen ocean water intrusions occur under minimal tidal mixing conditions and maximum diurnal inequalities at Admiralty Inlet (i.e., low turbulence and high exchange flow conditions). In addition, Admiralty Inlet experiences high ship traffic, and has been recognized as a prominent site for tidal energy extraction due to its strong tidal currents.

As a complement to high temporal resolution measurements at single location across the inlet, long-term measurements of high spatial resolution spanning the entire inlet are crucial for understanding circulation through Puget sound, improving navigation safety, and for tidal energy resource characterization.

Although the instrumentation and capabilities exist, the use of multiple moored instruments does not provide enough spatial resolution, and can become cost-prohibitive, as instruments need to be frequently recovered and redeployed for biofouling clearing, sensor maintenance, data retrieval, and changing batteries. Using instruments cabled to shore or to surface buoys can mitigate some of these problems, but this approach still limits where the instruments can be installed, and can become substantially costly and logistically complex. Continuous measurements from vessel mounted instruments provide the spatial resolution needed, but the use of dedicated research vessels for long periods of time can become cumbersome and impractically expensive. Vessels that sail the same route for extended periods of time pose an excellent cost-effective platform to obtain long time series of oceanographic variables across a large domain (Petersen 2014; Balfour et al. 2012). Such is the case of the Washington State Department of Transportation (WSDOT) Ferries, which run year round through the basins of Puget Sound.

The Washington State Department of Ecology (WSDOE) and WSDOT have partnered with the University of Washington Applied Physics Laboratory to implement and maintain a Ferry-Based Monitoring System of Puget Sound Currents. The aim of the project is to map the circulation in Admiralty Inlet and estimate the exchange of water between Puget Sound and the Strait of Juan de Fuca, to improve and calibrate water-quality models through Puget Sound. ADCPs have been installed on board the MV Kennewick and MV Salish ferries, and these continuously collect water velocities across Admiralty Inlet during the multiple daily runs of the ferries.

This paper presents flow velocity observations across Admiralty Inlet collected from the ferry-mounted ADCPs. Data from the first 4 years of operations (2014–2017) are analyzed to obtain the harmonic constituents of tidal currents across and through the depth of the inlet, and the first steps are taken to estimate residual currents and tidal power density from the data. Data collection details are given in Sect. 2, and data quality control and organization are presented in Sect. 3. Section 4 presents data analysis and results, including tidal currents harmonic analysis, estimations of residual currents, and estimation of tidal power density. Finally, conclusions are presented in Sect. 5.

2 Data collection

2.1 Ferry routes and ADCP settings

Admiralty Inlet is about 6 km wide with large bathymetric gradients in the across-channel direction. Figure 1 shows the location of the inlet within Puget Sound, and a detailed map

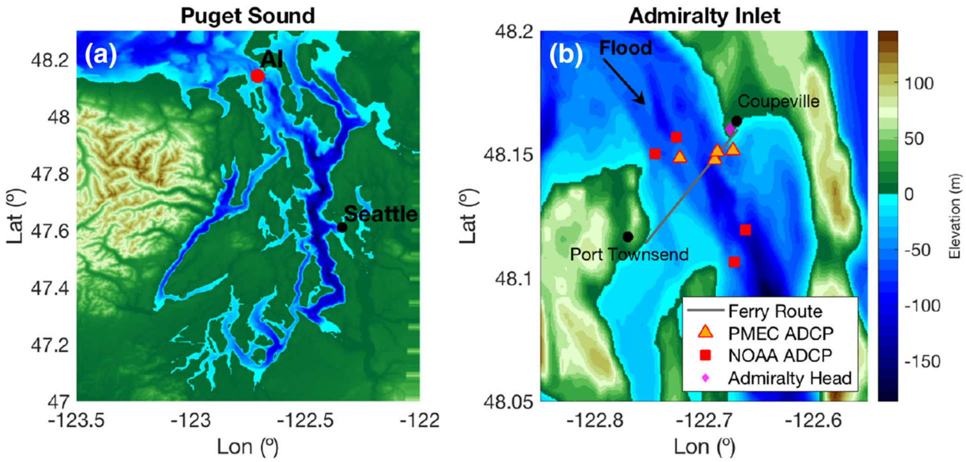

Fig. 1 **a** Map of Puget Sound, Washington, USA, colored by topo-bathymetry. Red dot shows Admiralty Inlet (AI) location within Puget Sound. **b** Map of Admiralty Inlet colored by topo-bathymetry. Grey line represents Port Townsend–Coupeville ferry route. Magenta diamond shows Admiralty Head location. Triangles and squares represent location of fixed acoustic Doppler current profilers (ADCPs) (color figure online)

Fig. 2 Down-looking ADCP installed in the hull of MV Salish

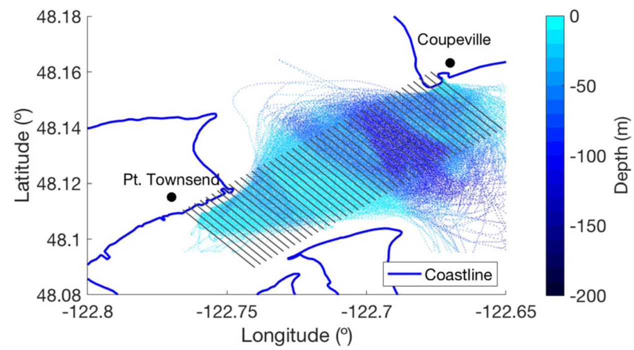

Fig. 3 Location of ferry-mounted ADCPs' velocity profiles measurements through Admiralty Inlet colored by location depth. Grey lines correspond to the along-channel edges of each grid cell used for data organization

of the Admiralty Inlet area colored by bathymetry, including the Port Townsend–Coupeville ferry route. The maximum depth along the ferry route is approximately 120 m.

Two down-looking acoustic Doppler current profilers (ADCPs) were installed on board MV Kennewick and MV Salish WSDOT ferries, which cross Admiralty Inlet between Port Townsend and Coupeville. The instruments were installed using a through-hull mount filled with fresh water and capped with a transparent polycarbonate window. A picture of the ADCP installed on board MV Salish is shown in Fig. 2. Each ADCP is installed near one of the ends of these symmetrical ferries.

The ADCPs, both 300 kHz RDI Workhorse Monitors, provide depth profiles of velocities in earth coordinates across the inlet since May 2014 (measurements are ongoing). For each ADCP, there are 60 bins of 2 m each, starting with a 2 m blanking distance from the instrument. The ADCPs are set to measure relative water velocities, bottom distance, and bottom-tracking velocities, which are later used to reconstruct true water velocities. Navigation velocities from the ferry's GPS are also available for data analysis. Data are sampled at 2 Hz and short time ensembles are calculated every 15 s. Both ferries run during the summer; only one of them runs the Admiralty Inlet route the rest of the year. Which one is running the route depends on other WSDOT Ferry schedules. The ferries are schedule to cross Admiralty Inlet 20 times each day.

Data collection is continuous, while the vessels are operational. All raw data collected from the ADCPs are stored locally on board the ferries. Short time ensembles (15 s) are uploaded daily to a public server and are available for download on the project website.[1] Available data include vertical profiles of velocity, bottom-track distance and velocity, navigation velocity, and ancillary ADCP data (including data necessary for quality control). In addition, bathymetry information from a Puget Sound Digital Elevation Model (NAVD88 datum) and tidal elevation predictions are also included for each ADCP measurement location and time. Figure 3 shows the spatial distribution of all vertical profiles of velocity collected by both ferry-mounted ADCPs through Admiralty Inlet (colored by depth). As seen in this map, there

[1] http://www.apl.washington.edu/ferriesforscience.

is significant scatter in data location, since the ferry does not take the exact same route at every crossing.

2.2 Additional data sets

Two additional data sets are used to test the accuracy of the data collected by the ferry ADCPs. These data sets provide flow velocities from fixed bottom-mounted ADCPs at several locations through Admiralty Inlet, with deployments lasting up to 3 months.

The first data set, from the Pacific Marine Energy Center (PMEC), includes data from different deployments at selected locations across Admiralty Inlet aimed at characterizing its available tidal energy resource. These deployments were concentrated near Admiralty Head (north–east side of Admiralty). Five deployments are selected for comparison, whose locations coincide with the ferry crossings. The second data set, from NOAA's Center for Operational Oceanographic Products (CO-OPS), includes velocity data from four ADCPs deployed in the vicinity of Admiralty Inlet in the summer of 2016. These deployments were part of NOAA CO-OPS effort to survey Puget Sound currents to update tidal current predictions, and to support future hydrodynamic models of the area. A summary of these deployment details is presented in Table 1. The location of the instruments from both data sets is shown in Fig. 1b.

In addition, ferry data will also be compared with data from the National Renewable Energy Laboratory Tidal Energy Atlas (Haas et al. 2011; Sutherland et al. 2011). This data set provides tidal current harmonics (eight) from depth-averaged flow velocities estimated from an ROMS numerical model of the area at a 350 m resolution in average (Haas et al. 2011; Sutherland et al. 2011).

3 Data processing

3.1 Quality control

All velocity data captured by the ferry ADCPs are processed to remove low-quality measurements. Data that do not meet the quality standards are removed from the set and are not considered in the subsequent analysis. The following criteria are applied to the entire ferry-based data set:

- Bottom-track return from at least two (out of four) ADCP beams is necessary, any less results in removal of the entire velocity profile.
- Remove any data collected deeper than the bottom-track return of each velocity profile
- Remove first five bins of data due to acoustic interference (ringing and bubbles) near ferry hull (Nauw et al. 2014)
- Set the following thresholds:

Table 1 Additional deployments and sampling parameters at Admiralty Inlet

Institution	PMEC					NOAA			
Instrument	RDI Workhorse 300 kHz			Nortek AWAC 600 kHz		RDI Workhorse 300 kHz			
Station	SS03a	SS01a	SS01b	SS03b	SS01c	PUG1619	PUG1620	PUG 1623	PUG1624
Lat (°)	48.1521	48.1509	48.1477	48.1515	48.1486	48.1063	48.1193	48.1501	48.1569
Lon (°)	− 122.6954	− 122.6877	− 122.6903	− 122.6738	− 122.7221	− 122.6725	− 122.6623	− 122.7454	− 122.7260
Deployment	4/9/09	5/20/09	11/12/09	11/10/10	2/13/11	6/18/16	6/19/16	6/19/16	6/21/16
Recovery	5/19/09	8/3/09	1/29/10	2/10/11	5/9/11	8/21/16	8/20/16	8/21/16	8/21/16
Ensembles (s)	600	30	45	60	60	360	360	360	360
Depth (m)						64.1	101	61.9	66.5
Nbins	61	51	59	40	40	48	28	46	48
First bin (m)	4.6	3.6	3.6	1.2	1.2	10.2	39.2	12.8	14.1
Top bin (m)	64.6	53.6	61.6	40.2	40.2	57.2	66.2	57.8	61.1
Δz (m)	1	1	1	1	1	1	1	1	1

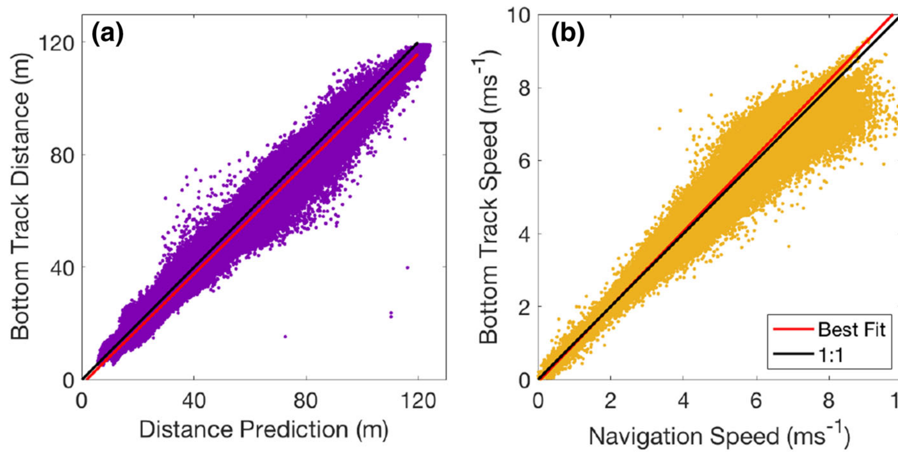

Fig. 4 **a** Bottom-track distance prediction from Puget Sound digital elevation model corrected by tidal elevation (x-axis) vs. ADCP measured bottom-track distance (y-axis), and **b** GPS ferry navigation velocities (x-axis) vs. ADCP bottom-track velocity (y-axis). Red lines correspond to data best-fit, and in black is the 1:1 line (color figure online)

- Minimum correlation: 35, established using spurious directions of tidal currents
- Absolute velocity: 7 ms^{-1}, established using the ambiguity velocity of the original ADCP settings
- Error velocity (vertical): 1 ms^{-1}, established empirically
- Maximum true water velocity magnitude: 4 ms^{-1}

The application of these strict quality controls removes more than half of the measured velocity profiles. Some of the causes of low-quality measurements are: (1) ferry propeller bubbles interfere with ADCP measurements during every other crossing. The ferries move back and forward at each crossing and the ADCPs are installed near one of the ferry propellers, and hence, for every other crossing, bubbles from one of the ferry propellers pass under the instrument. These bubbles interfere with the acoustic back-scattering on which Doppler profilers rely for estimating water velocity. (2) Marine growth accumulates on the ADCP glass window, though it is regularly cleared and coated with zinc oxide to inhibit biofouling. (3) Vessel speeds, sometimes, exceed the absolute velocity threshold, especially when they take longer routes due to conflicting vessel traffic.

The accuracy of bottom-track distance and bottom-track velocities is tested by comparing them to the Puget Sound Digital Elevation Model (corrected for tidal elevation) and to the GPS-based vessel navigation speed, respectively. Figure 4 shows scatter plots of both quantities, showing a good agreement between the different data sets, despite the observed scatter. For the bottom-track distance, the best-fit slope is 0.98 with a 1.57 m intercept, while, for the ferry speed, the best-fit slope is 1.03 with a -0.06 ms^{-1} intercept. The root-mean-square error for both data sets is 2.9 m and 0.2 ms^{-1}, respectively. Note that these plots and calculations only consider data that passed the quality control process. A bias in the bottom-track velocities will directly impact the water velocity estimation; a positive bias would manifest as water velocities looking similar to vessel velocity magnitude and direction.

3.2 Spatial gridding and generation of time series

Quality controlled data are organized in a horizontal and vertical grid across the inlet, which accounts for spatial variability between ferry crossings and tidal elevation changes, respectively. The inlet is gridded into 44 cells each 200 m in the across-channel direction, and into fixed 2 m vertical cells (within each horizontal cell) extending deeper than the deepest measurement captured by the ADCPs (150 m per instrument setup).

The horizontal grid resolution is determined considering ADCP ensemble average times and velocity gradients in the cross-channel direction. The ADCPs were set to produce 15 s ensemble-averaged velocities to reduce the Doppler noise inherent to the measurement method. For an average ferry navigation speed of 6 ms^{-1}, each ADCP velocity ensemble covers 90 m horizontally; this distance sets the minimum grid cell width. The previous studies in Admiralty Inlet (Polagye and Thomson 2013; Palodichuk et al. 2013) showed strong spatial gradients on the order of 200 m, especially in the cross-channel direction. The grid cell width is chosen to be as big as possible while still capturing these 200 m changes. The analysis focuses on cross-channel variations, and hence, only one horizontal grid cell is considered in the along-channel direction (3 km long to capture most of the ferry crossings).

The horizontal grid begins south of Port Townsend (adding 2 km to the width of the inlet) and ends south of Coupeville. Grey lines in Fig. 3 show the edges of each grid cell. The GPS horizontal location of each measurement is used to map the velocity profiles into the grid. The vertical grid zero coincides with the NAVD88 datum zero at this location (Puget Sound digital elevation model datum). ADCP's vertical bin locations are referenced to NAVD88 datum using

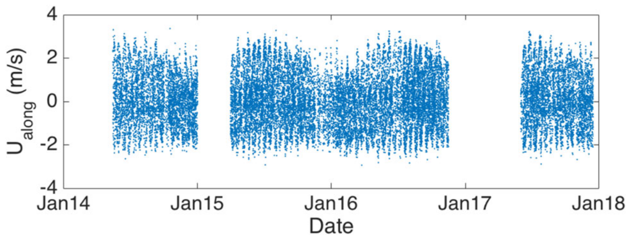

Fig. 5 Example of a non-uniform time series of along-channel velocity from ferry-based measurements within a single grid cell

the tidal elevation prediction (referenced to NAVD88 too) at each measuring time before vertical grid organization. Standard deviation of depth within each grid cell ranges between 0.8 m (in the shallower areas of the inlet) and 18 m (where the strong cross-channel bathymetry gradients are observed).

Finally, data within each grid cell constitute a non-uniform time series of horizontal velocities across Admiralty Inlet at different depths. Figure 5 shows a time series example of along-channel velocity from a grid cell located-mid-channel, about 20 m below the free surface. In this figure, the gaps in data correspond to low-quality measurements. Here, the tidally modulated behavior of currents is also observed.

3.3 Sample bias test

The ferries that cross Admiralty Inlet run only during the day, so that there are no ADCP measurements during the night, and two ships cover the inlet during the summer, resulting in more measurements during summer time than during the rest of the seasons. A consequence of this change in schedule is sample bias, in which some tidal stage can be preferentially measured. For example, more measurements can occur during low tides than during high tides (or the opposite), and more samples can occur during ebbs than during flood currents. Here, sample bias is tested using the valid gridded data time stamps.

To test the sample bias at each grid cell, tidal elevation and tidal currents are reconstructed at the time stamps of valid ferry-based measurements within each grid cell using harmonic analysis. The use of reconstructed time series for sample bias testing is preferred, since no tidal elevation data are collected by the ferry ADCPs. Furthermore, water velocities from the ferry ADCPs have uncertainties from instrument Doppler noise and from the gridding process that can influence the distribution of the sampled tidal stages.

Harmonic constituents for tidal elevation and tidal currents obtained from one of the NOAA bottom-mounted ADCPs (PUG1624) are used for the harmonic time-series reconstruction. In addition, uniform time series (Δt = 10 min) of tidal elevation and tidal currents are reconstructed using the same harmonic components for the same period of time covered by the valid time stamps. These uniform time series represent what would have been measured by a fixed platform ADCP at each grid location. Following the reconstruction, the probability distributions of both non-uniform and uniform-reconstructed tidal elevation and tidal currents are estimated and compared to the assess sample bias.

Figure 6a, b shows the estimated probability distributions at one grid cell. Figure 6c, d shows Q–Q (quantile–quantile) plots comparing the quantiles of the estimated distributions. A two-sample Kolmogorov–Smirnov test was also applied to compare both types of reconstructed time series (uniform and non-uniform). The test results indicate that the time series do not come from exactly the same distribution. Although the distributions from the ferry sample times have some noise, no large differences are observed when compared to the distribution from uniformly sampled data. The same behavior is observed in all the tested grid cells. The probability skewness for low tide, around −2 m, is also observed in the distributions of free-surface elevation measured by the additional bottom-fixed ADCPs included in this study (see Table 1), and is explained by the mixed semi-diurnal tidal regime of Admiralty Inlet. Root-mean-square error (RMSE) between the reconstructed time series at the valid ferry-based sample times is 0.02 m for tidal elevation and 0.03 ms^{-1} for the along-channel velocities.

Sample bias in tidal components phase is also tested. Distribution of sampled tidal phase for the four of the most significant tidal components (M_2, N_2, K_1, and O_1) at this site is close to uniform. However, the phases of the S_2 component (of 12 h period) are not uniformly sampled, because the ferries do not run at night (Codiga and Aurin 2007).

4 Data analysis

4.1 Tidal current harmonic analysis

Tides dominate the circulation signal at Admiralty Inlet; thus, the first application of the cleaned and organized data set is to capture the tidal harmonic constituents of the currents. Harmonic analysis of binned, non-uniform time series of horizontal currents is performed using UTIDE (Codiga 2011), which is a unified tidal analysis and prediction model. UTIDE performs harmonic analysis of two-dimensional time series with irregular sample times, such as the time series created in the griding process. Harmonic analysis is also applied to the fixed ADCP data for comparison.

Ferry measurements are ongoing, and thus, the data set is continuously growing. Before performing harmonic analysis to the entire data set, sensitivity to the length of the gridded non-uniform time series in the harmonic analysis results is studied. Here, the accuracy and convergence of the harmonic analysis results are tested as more valid samples are added to the data set. Using data from a single grid cell at a single

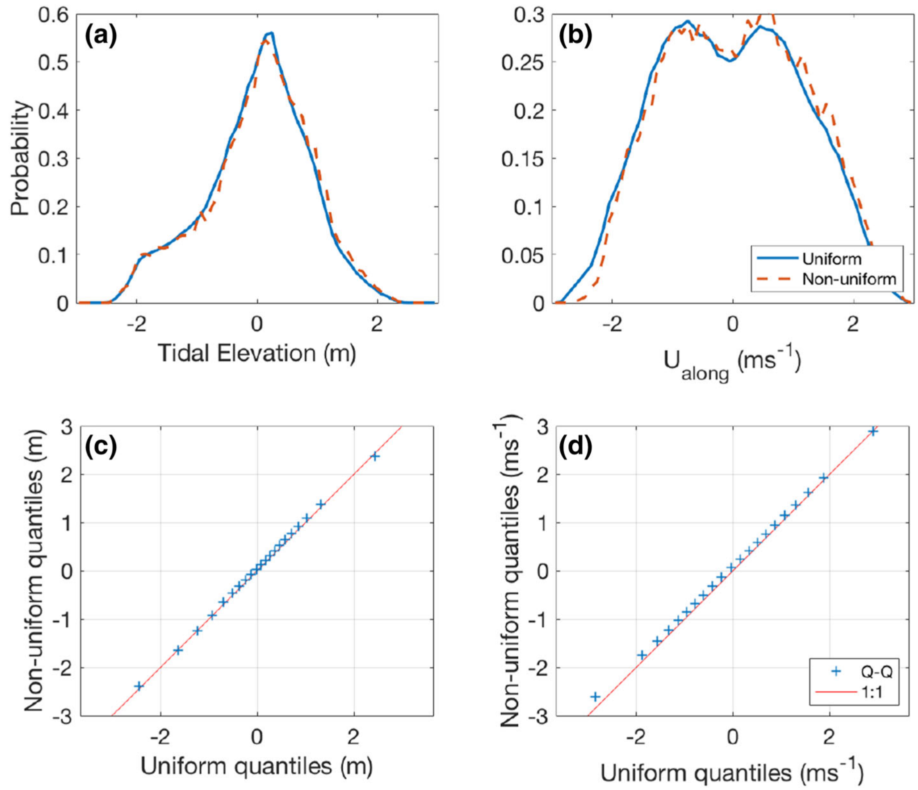

Fig. 6 Probability distribution of **a** tidal elevation, and **b** along-channel velocity. Blue lines represent distributions from a uniformly sampled time series, while the red dashed line represents the distribution from a non-uniformly sampled time series. **c**, **d** Show Q–Q plots comparing both distributions for both tidal elevation and along-channel velocity (color figure online)

depth, harmonic analysis is applied to a valid velocity time series of increasing length. For each test, one extra month of already collected data is added, which, for some cases, means adding a reduced amount of new valid data or none at all. Figure 7 shows the harmonic analysis test results for the M_2 tidal current semi-major amplitude (which is the dominant harmonic at Admiralty Inlet) together with the confidence interval results from UTIDE. As seen in this plot, the uncertainties decrease significantly when more than 10,000 valid data points are used in the analysis. When more than 20,000 valid samples are used, the M_2 amplitude has converged and the confidence interval width remains constant. The confidence interval width is fitted to the amount of valid samples N, and it is found to agree very well to the typical standard error definition of $1/\sqrt{N}$. The same sensitivity analysis is performed to four other tidal harmonics (S_2, N_2, K_1, and O_1), and the same results are found (not shown); amplitudes converge and confidence intervals decrease in width.

Based on this convergence, the ferry-based ADCP measurements to-date are sufficient to resolve the tides. Harmonic analysis is applied at all horizontal and vertical grid cells to obtain a spatial distribution of the tidal current harmonics across the inlet.

At least the five most energetic tidal current components are recognized from the data set (M_2, K_1, S_2, N_2, and O_1). Each one of these components contributes more than 1% of the kinetic energy in the tidal currents, and together account for $\sim$ 93% of the kinetic energy (M_2 contains $\sim$70% of the energy, K_1 $\sim$10%, S_2 $\sim$5%, K_1 $\sim$4%, and O_1 $\sim$4%, respectively). Up to 30 constituents are solved across the inlet [with a signal-to-noise ratio higher than 10 (Codiga 2011)], with the higher number of constituents solved at mid depth in the middle of the channel. However, the additional solved components contribute less than 1% of the energy, and, thus, are not presented here.

Figures 8, 9 show the vertical distribution of the M_2 and K_1 tidal current harmonic component ellipse parameters across the inlet. Large spatial variability is observed in the semi-major amplitudes of the M_2 tidal current component, probably related to bathymetric features of the area (headland and sill) (Lavelle et al. 1988; Sutherland et al. 2011; Yang and Khangaonkar 2010). Lower amplitudes (below 0.5 ms^{-1}) are observed in the shallow area to the south of Port Townsend. Stronger amplitudes (above 1 ms^{-1}) are observed through the water column at mid-channel, where a deeper and narrow channel exists. A similar pattern is observed for the K_1 component semi-major amplitudes, with stronger flows mid-channel. For both components, semi-minor amplitudes are low (less than 0.1 ms^{-1}) indicating low cross-channel flows, and ellipse orientation across the inlet align with the main channel orientation (approximately north-west). However, uncertainties in the harmonic analysis results (not shown) are large in the shallower areas south of Port Townsend and

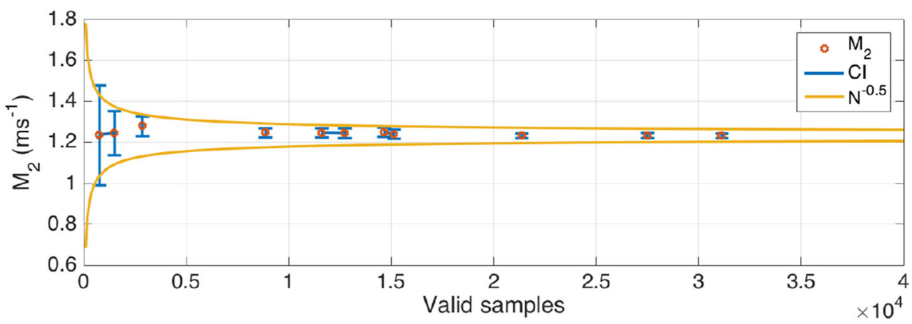

Fig. 7 Convergence of harmonic analysis results with number of valid samples. M_2 tidal current amplitude in red circles, confidence intervals in blue bars, and $1/\sqrt{N}$ curve in yellow (color figure online)

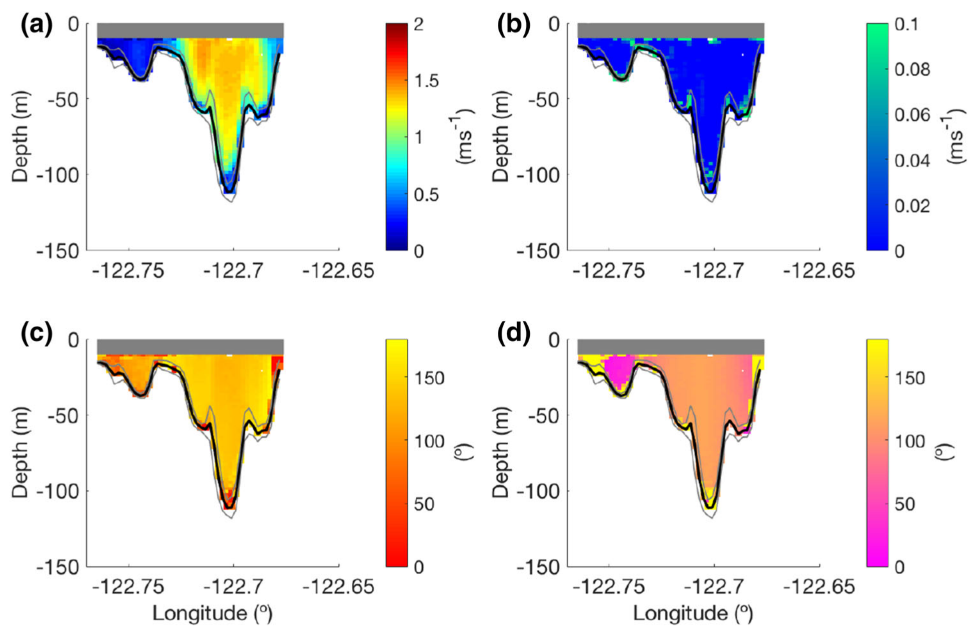

Fig. 8 Harmonic analysis results across Admiralty Inlet for M_2 tidal current: **a** semi-major amplitude in ms^{-1}, **b** semi-minor amplitude in ms^{-1}, **c** ellipse orientation in degrees, and **d** Greenwich phase in degrees. Grey area represents water column depth not covered by the ferry measurements (down to $z = -10$ m). Black line shows mean depth at each grid cell and grey lines show $\pm$ one standard deviation from the mean depth

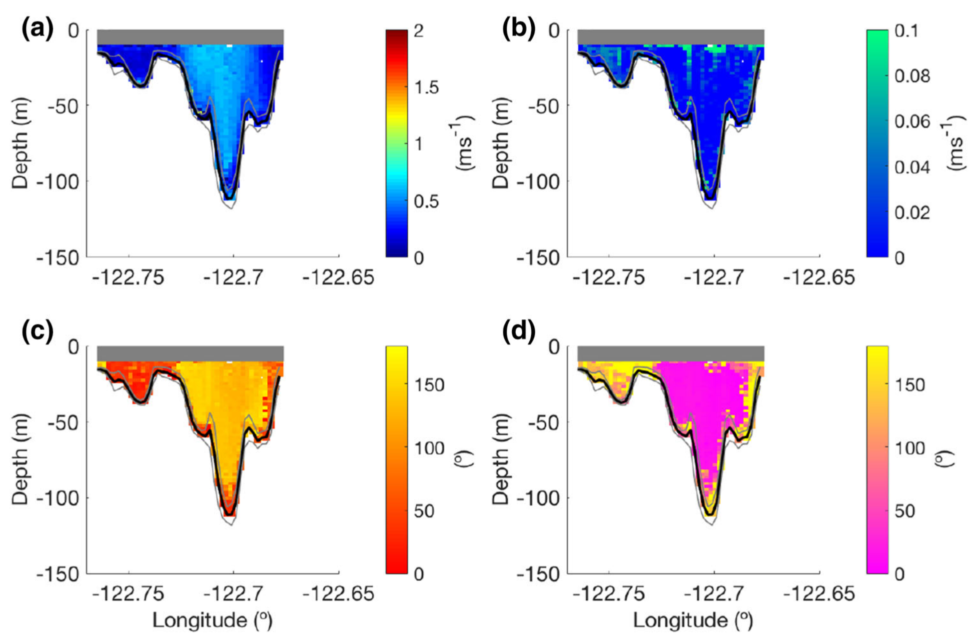

Fig. 9 Harmonic analysis results across Admiralty Inlet for K_1 tidal current: **a** semi-major amplitude in ms^{-1}, **b** semi-minor amplitude in ms^{-1}, **c** ellipse orientation in degrees, and **d** Greenwich phase in degrees. Grey area represents water column depth not covered by the ferry measurements (down to $z = -10$ m). Black line shows mean depth at each grid cell and grey lines show $\pm$ one standard deviation from the mean depth

close to the bottom in the deeper channel, because currents are weaker and less data are available at those locations.

Comparisons are made with harmonic analysis results from the additional bottom-fixed ADCP measurements and from the Tidal Energy Atlas data. Since the Tidal Energy Atlas only provides harmonic results from depth-averaged tidal currents, harmonic analysis is applied to depth-averaged currents from the ferry-based measurements and from the fixed ADCPs.

Not all fixed deployments covered the same portion of the water column, and the ferry-based measurements do not cover the top 10 m of the water column (these measurements were removed in the quality control process). Following a sensitivity analysis of the portion of the water column used in defining the depth-averaging the currents, using the middle 55% of the water column (from 15 to 70%) results in the same depth-average values as if the whole water column is used (at Admiralty Inlet). The analysis is based on data from PMEC SS01b station data. The M_2 semi-major tidal current amplitude from 100% depth-averaged time series is 1.388 ms^{-1}, while such amplitude is 1.392 ms^{-1} when using the 55% portion of the water column. Hence, a 55% column (from 15 to 70%) is used to define the depth-average currents for the comparison of all fixed deployments and for the ferry-based measurements with the Tidal Energy Atlas Results.

Figure 10 shows M_2 depth-averaged tidal current ellipses from the different data sets, and Fig. 11 shows depth-averaged tidal current ellipses for the remaining four most energetic components. Note that, at some grid cells, there is no ellipse available, because there were not enough data to obtain a valid result. In general, results from ferry measurements align with those from the bottom-fixed ADCPs and with those form the Tidal Energy Atlas in the deeper mid-section of the channel. Results from the ferries show slower currents than those from the fixed ADCPs, but higher than those from the Atlas. M_2 tidal current amplitudes from the Tidal Energy Atlas are always smaller than those from bottom-mounted ADCPs, because simulation results used to estimate the tidal currents harmonics were likely biased low when compared to field measurements (Thyng et al. 2013). At the mid-channel section, grid cells contain above 15,000 valid measurements, and smaller uncertainties are observed in the harmonic analysis results as demonstrated in Fig. 7. Table 2 shows depth-averaged harmonic analysis results for a grid cell centered at 48.1359°N–122.7009°W (cyan dot in Fig. 10). Tables 3, 4 show root-mean-square errors (RMSE) between depth-averaged ferry-based harmonic analysis results and NREL Tidal Energy Atlas results, and between PMEC station SS01c depth harmonic analysis results and the results from the closest grid cell, respectively.

A large difference is observed in both semi-major amplitude and ellipse orientation near Admiralty Head for all presented components (see Fig. 12). Large spatial gradients in the tidal currents have been observed here and likely are related to flow separation caused by the headland (Polagye and Thomson 2013; Palodichuk et al. 2013). These gradients are illustrated by the Tidal Energy Atlas ellipses, which rapidly increase in magnitude near the PMEC ADCPs locations. South of the headland, the currents reduce as they turn, as shown by the PMEC ellipse towards the north–east. In this area, the ferry ellipses follow the same trend, but are significantly smaller. This discrepancy can be explained by spatial variability occurring within the grid cells, which are 3 km long in the along-channel direction, and, thus, do not capture small spatial gradients (especially in the along-channel direction).

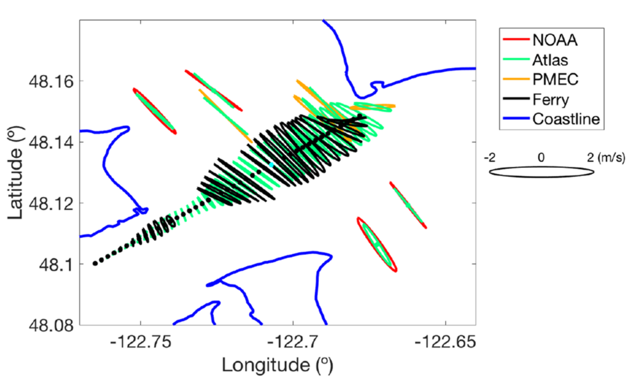

Fig. 10 M_2 depth-average tidal current ellipses from different data sets. In black from ferry-mounted ADCPs, in red from NOAA-CO-OPS ADCPs, and in yellow from PMEC ADCPs. Green ellipses are from NREL Tidal Energy Atlas at the ferry data grid, NOAA-CO-OPS, and PMEC locations. Cyan dot represents location of grid cell used for power estimations (color figure online)

4.2 Residual flow

The estimation of mean circulation and the estuarine exchange flow between Puget Sound and the ocean requires long-term characterization (for several seasons) of the currents across Admiralty Inlet. Here, gridded ferry-based measurements are tested to capture sub-tidal residual currents and are compared to co-temporal measurements from a fixed bottom-mounted ADCP. The approach here-in uses a simple long-term average and, thus, does not explicitly separate tidal asymmetry from exchange flow. The long-term mean along-channel velocity component through the water column, a proxy for average residual flow, is explored. Estimations of mean flow velocities across the inlet (using the entire ferry data set) and its corresponding standard error are shown in Fig. 13. Interesting spatial circulation patterns are observed. Mid-channel flow is landward dominated, while the area near Admiralty Head is ocean-ward dominated, as previously observed by Polagye and Thomson (2013). Stronger inflow is observed in the deeper portion of the channel, as expected for denser

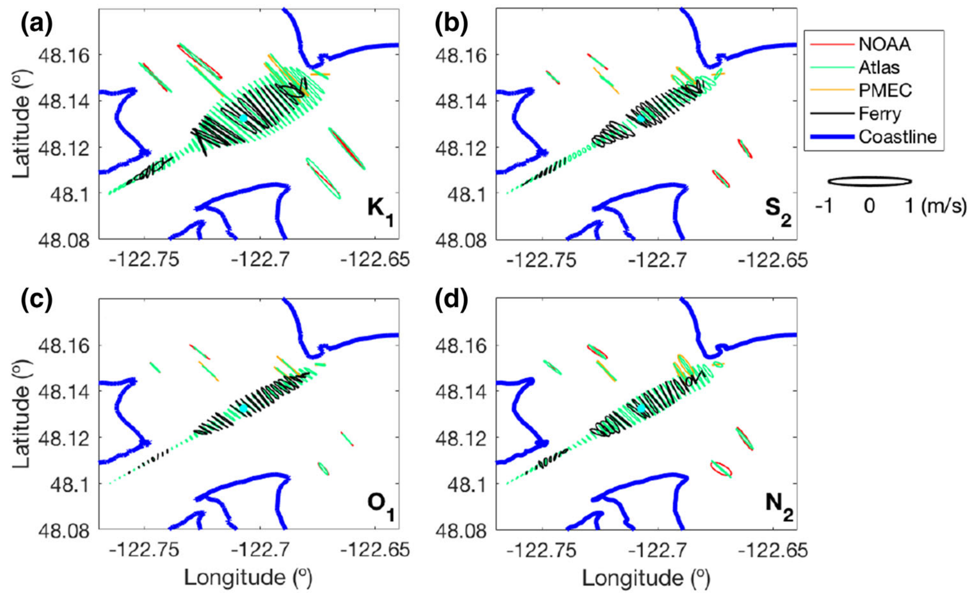

Fig. 11 Depth-average tidal current ellipses from different data sets for: **a** K_1, **b** S_2, **c** O_1, and **d** N_2 tidal current components. In black from ferry-mounted ADCPs, in red from NOAA-CO-OPS ADCPs, and in yellow from PMEC ADCPs. Green ellipses are from NREL Tidal Energy Atlas at the ferry data grid, NOAA-CO-OPS, and PMEC locations (color figure online)

Table 2 Depth-averaged ferry-based harmonic analysis results at grid cell centered at 48.1359°N–122.7009°W

Component	Semi-major axis (ms^{-1})	Semi-minor axis (ms^{-1})	Orientation (°)	Phase (°)
M_2	1.21	0.02	139.30	116.69
K_1	0.55	0.00	142.01	15.60
S_2	0.32	0.03	139.81	139.53
O_1	0.31	0.03	133.87	345.25
N_2	0.27	0.01	135.19	81.70

Table 3 Root-mean-square errors between depth-averaged ferry-based harmonic analysis results and NREL Tidal Energy Atlas results

Component	Semi-major axis (ms^{-1})	Semi-minor axis (ms^{-1})	Orientation (°)	Phase (°)
M_2	0.27	0.06	31.85	42.64
K_1	0.20	0.03	25.44	47.26
S_2	0.11	0.05	16.50	33.46
O_1	0.07	0.04	27.24	97.47
N_2	0.06	0.02	33.36	62.38

Table 4 Root-mean-square errors between ferry-based and PMEC station SS01c harmonic analysis results

Component	Semi-major axis (ms^{-1})	Semi-minor axis (ms^{-1})	Orientation (°)	Phase (°)
M_2	0.28	0.03	6.97	8.43
K_1	0.14	0.11	12.50	11.21
S_2	0.10	0.09	12.51	11.55
O_1	0.08	0.04	14.69	234.81
N_2	0.07	0.04	11.57	230.27

ocean water. No outflow is observed in the upper water column, since that portion is not well captured by the ferry-based measurements.

The mean flow magnitudes generally are greater than those observed during fixed bottom-mounted deployments. Mean velocity profiles are estimated at one of the mid-channel grid cells (centered at 48.1359°N–122.7009°W) and at NOAA station PUG1624 (48.1569°N–122.7260°W). Both locations are aligned, but are located 3 km apart in the along-channel direction. Ferry-based velocities from June 21 to August 21 2016 are used for time-averaging to match collection dates from NOAA station PUG1624. Figure 14 shows the vertical profiles of mean velocities from the respective data sources. The profile from the ferry-based measurements shows mean

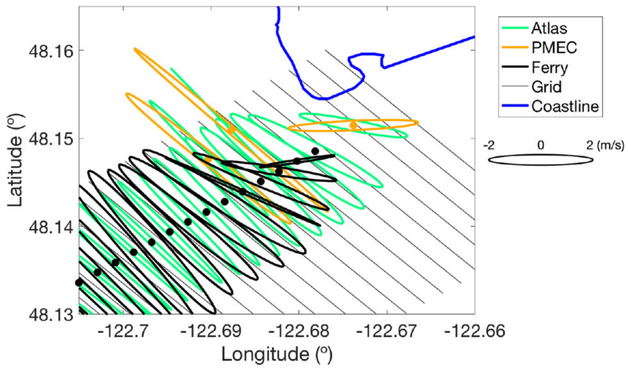

Fig. 12 Zoom in version of M_2 depth-average tidal current ellipses from different data sets. In black from ferry-mounted ADCPs and in yellow from PMEC ADCPs. Green ellipses are from NREL Tidal Energy Atlas at the ferry data grid and PMEC locations. Dots represent the ellipses center location and grey lines represent the grid edges (color figure online)

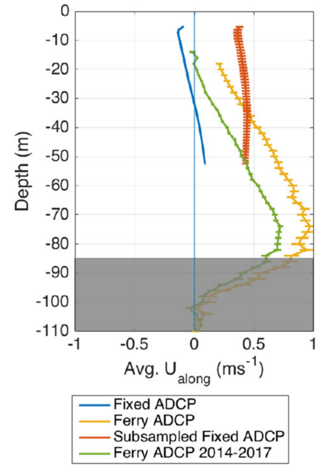

Fig. 14 Time-averaged velocity profile from fixed bottom-mounted ADCP measurements at station PUG1624 (blue), from summer 2016 ferry-based measurements within a single grid cell (yellow), from sub-sampled fixed bottom-mounted ADCP measurements (red), and from the entire ferry-based time series at the same grid cell (green). Horizontal lines represent standard error on estimating the time-average values. Grey covered area corresponds to measurements below the mean grid cell depth (color figure online)

flows an order of magnitude stronger; no outflow (negative, towards the ocean) is observed in the upper water column, since no ferry-based data are available there. However, the expected flow pattern is observed in the lower portion of the water column, where stronger positive (landward) flows are observed towards the bottom. The large differences between both mean flow estimates might be explained by the spareness of the ferry-based time series. To test this hypothesis, the bottom-fixed data are sub-sampled down to the spareness of the valid ferry-based measurements (i.e., using only the valid collection times from the ferry data). The residual currents from the sub-sampled time series increase and are of the same order of magnitude of the ferry-based residual currents (considering only the summer months), consistent with the sampling hypothesis.

For real-time operational purposes, such as identifying ocean water intrusions that might affect water quality, time series of residual flows are needed (Deppe et al. 2018). Here, the capability of the ferry-based data set to provide such real-time information is explored. A low-pass filter of 40 h half-amplitude period is applied to along-channel velocity time series, at different depths, to remove the tidal currents and retain the residual currents (Alessi et al. 1985; Polagye and Thomson 2013; Deppe et al. 2018). Residual flows are also estimated for the sub-sampled data from station PUG1624 as ground truth for the results from the ferry-based measurements. Figure 15 shows the results for a depth $\sim$ 35 m below the free surface. Large differences are observed in the residual flows estimated from the two different platforms. Large magnitude oscillations persist in the ferry data, and this indicates that such a filtering method is not suitable for the sparse ferry data set. Other authors have applied harmonic analysis to obtain tidal currents predictions, and estimated residual currents time series by removing the predictions from the measurements (Nauw et al. 2014). However, this approach requires resolving most of the tidal harmonic components, such that all tidal periods are removed from the measurements.

Fig. 13 **a** Map of time-averaged velocities using entire length of velocity time series within each grid cell, and **b** corresponding standard error of the time-averaged quantities

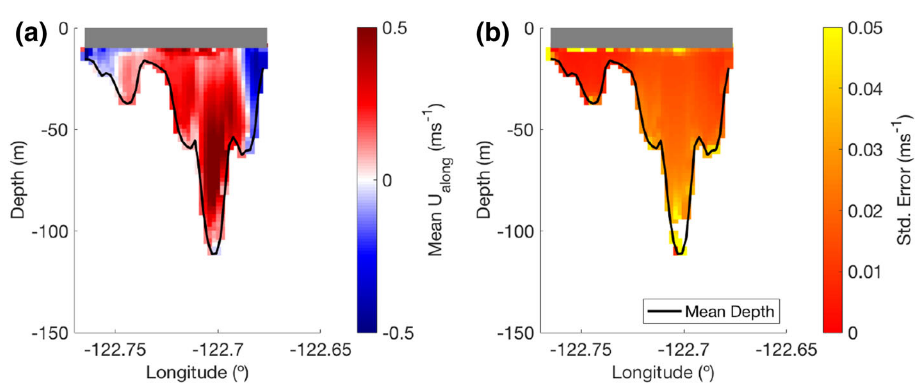

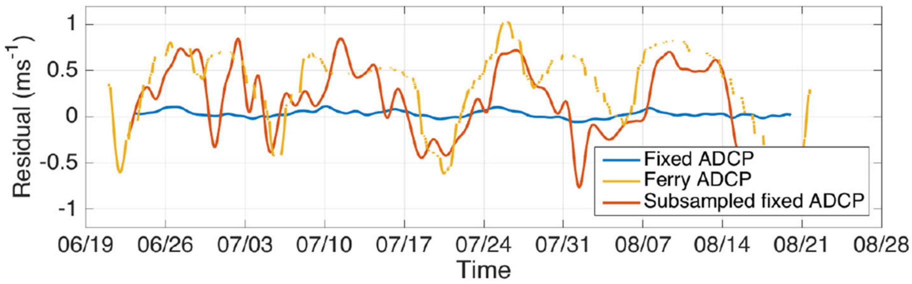

Fig. 15 Time series of residual currents from fixed bottom-mounted ADCP at NOAA station PUG1624 (blue), from ferry-based ADCP measurements within single grid cell (yellow), and from a sub-sampled bottom-mounted ADCP at NOAA station PUG1624 (red) (color figure online)

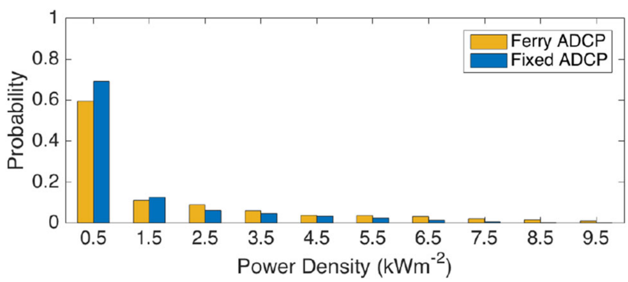

Fig. 16 Power density histograms using summer 2016 data: from fixed bottom-mounted ADCP measurements (blue, NOAA PUG1624), and from ferry-based measurements within a single grid cell (yellow) (color figure online)

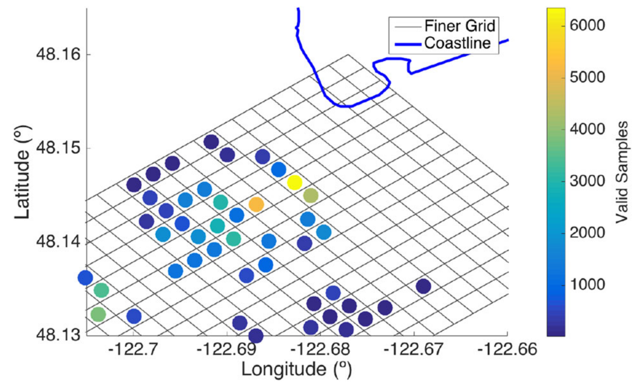

Fig. 17 Small grid example (200 × 200 m^2) near Admiralty Head area. Colored dots represent amount of valid samples within each grid cell (color figure online)

4.3 Tidal energy resource

Admiralty Inlet has been previously identified as feasible site for tidal energy extraction. A tidal energy demonstration project was a proposed by Snohomish County Public Utility District at the north–east part of Admiralty Inlet, which considered the installation of two OpenHydro turbines, but the project was discontinued in 2014 due to funding challenges (Snohomish County Public Utility 2014).

The available, but not necessarily extractable, kinetic energy flux is typically described by the local power density (Garrett and Cummins 2005), which depends on the cube of the water velocity **u** and the water density ρ, such that:

$$P = \frac{1}{2}\rho \mathbf{u}^3. \tag{1}$$

Here, gridded ferry-based measurements are used to estimate the local power densities throughout Admiralty Inlet and are compared to co-temporal estimates from a fixed bottom-mounted ADCP.

Power density estimates at a single grid location (centered at 48.1359°N–122.7009°W, cyan dot on Fig. 10) are compared with co-temporal data from NOAA station PUG1624 (48.1569°N–122.7260°W). These are the same grid and fixed bottom-mounted ADCP stations used for exchange flow calculations in Sect. 4.2. Again, ferry-based velocities from June 21 to August 21 2016 are used in the calculations to match collection dates from station PUG1624. Figure 16 shows histograms of power density estimated 35 m below the free surface. The two probability distributions agree well, except at low power densities (0.5 kWm^{-2} bin). Under these low power density conditions, hydrokinetic turbines would not be operational, so this mismatch is not significant. Average power density within the summer months is estimated to be 1.8 kWm^{-2} from the ferry-based measurements, compared with 1.1 kWm^{-2} from the NOAA station measurements, which corresponds to a 60% difference in average power density. Considering power estimates at PUG1624 only at the times of valid ferry-based samples, the RMSE between both time series of power is 1 kWm^{-2}.

5 Conclusions and discussion

Long-term observations of currents across Admiralty Inlet from ferry-mounted acoustic Doppler current profilers (ADCPs) are quality controlled, organized, and tested to capture tidal current harmonics and residual flows through the inlet. Data are collected by two ADCPs mounted on board two ferries that cross Admiralty Inlet about 20 times a day. All measurements are organized into a horizontal and vertical grid, which results in non-uniform time series of velocities across the entire inlet.

Despite the dramatic reduction of data coverage after quality control, the remaining data successfully capture the main tidal current harmonics. New maps of tidal currents harmonics are now available across and through the depth of Admiralty Inlet. Harmonic analysis shows sharp gradients in tidal current amplitudes across the inlet, probably related to the bathymetric features of the inlet (Lavelle et al. 1988; Sutherland et al. 2011; Yang and Khangaonkar 2010). Stronger currents are observed mid-channel and towards the north–east end of the inlet, while slower currents are observed in the enclosed shallow area south of Port Townsend.

Harmonic analysis results agree well with those from fixed bottom-mounted ADCPs towards mid-channel in terms of ellipses amplitude and orientation. Less agreement is found towards the shallow areas of the inlet and closer to the shore, specially near Admiralty Head. These differences might be explained by large horizontal gradients in the currents observed there, which are obscured by the choice of grid.

A higher resolution grid could be applied in the along-channel direction to capture the currents spatial gradients near Admiralty Head. Two or three along-channel grid cells ($\sim$ 1 km long) would probably have enough valid data points to ensure harmonic analysis convergence; however, for capturing these sharp gradients, a much finer grid resolution would be needed. Figure 17 shows an example of a smaller grid of 200×200 m^2 resolution near Admiralty Head, in which most of the grid cells have less than 6000 valid samples (which is not enough for convergence according to results, as shown in Fig. 7). The latter suggest that another method, such as the station keeping method from Palodichuk et al. (2013), should be better suited to map those areas at higher resolution. Future investigations could also explore a different vertical grid method. For example, a stretched vertical coordinate, similar to what is used in oceanographic numerical models, could be used instead of a fixed vertical grid. This method was applied by Codiga and Nehra (2012) to ferry-based ADCP velocity measurements to obtain a more uniform distribution of measurements within each vertical grid, thus, improving their tidal and residual flow calculation statistics.

A new cross-section map of mean flow velocities is obtained from the ferry-based measurements. This map exhibits the spatial circulation pattern across Admiralty Inlet, where stronger inland mean flows occur in the deeper portion of the channel, while stronger outflow occurs near Admiralty Head. A first attempt to estimate time series of residual currents from ferry-based measurements by filtering out the tidal currents is presented; however, the temporal method fails due to the sparseness of the gridded velocity time series. The ferry-based measurements are not suitable for real-time estimations of exchange flows, and no improvement is found relative to the existing forecasting method of Deppe et al. (2018).

The mean flow velocities result suggest that the ferry-based data are sufficient to determine the spatial patterns of residual flow through Admiralty Inlet, but that it will be difficult to use this data for quantitative estimates of residual currents or resolving changes in estuarine exchange flows. The data are still of great value, because the spatial patterns obtained could be used to guide the placement of more continuous monitoring of residual flows.

Differences between average power density estimates from ferry-based data and from bottom-fixed ADCP data might be explained by the true spatial variability in the tidal currents, i.e., stronger currents occur within the studied grid cell. Following the cubed velocity, a small increase in velocity leads to a large increase in power density.

Ferry-based data provide new insights on the spatial distribution of currents through Admiralty Inlet. Results obtained so far could improve tidal currents maps through Admiralty Inlet, estimates of the tidal energy resource available, and numerical hydrodynamic models of the area. Measurements are ongoing, and thus, better estimates of tidal current harmonic components will be available over time, which may reduce the need for large spatial bins to accumulate a sufficient number of data points. New methods for estimating residual flows from sparse data sets need to be explored to estimate the total exchange flow through Admiralty Inlet.

Acknowledgements The authors would like to thank the support of Washington State Department of Transportation Ferries, in particular Mark Scoville and Cotty Fay. The authors acknowledge NOAA, PMEC, and Dr. Kevin Haas for facilitating the additional data sets used in this investigation, as well as Alex de Klerk for design and implementation of data acquisition systems. Maricarmen Guerra thanks the support of Fulbright and Becas Chile doctorate fellowship programs. This project has been funded wholly or in part by the United States National Estuary Program funded by the US Environmental Protection Agency under assistance agreement PC00J20101 to Washington Department of Ecology. The contents of this document do not necessarily reflect the views and policies of the Environmental Protection Agency, nor does mention of trade names or commercial products constitute endorsement or recommendation for use.

References

Alessi C, Beardsley R, Limeburner R, Rosenfeld L, Lentz S, Send U, Winant C, Allen J, Halliwell G, Brown W, Irish J (1985) Code-2: moored array and large-scale data report. Tech rep 85–35, Woods Hole Oceanographic Institution

Balfour C, Howarth M, Jones D, Doyle T (2012) The design and development of an Irise Sea Passenger-Ferry-Based oceanographic measurement system. J Atmos Ocean Technol 30:1226–1239

Codiga D (2011) Unified tidal analysis and prediction using the UTide Matlab functions. Tech. Rep. 2011-01, Graduate School of Oceanography, University of Rhode Island, Narragansett, RI

Codiga D, Aurin D (2007) Residual circulation in eastern long island sound: observed transverse-vertical structure and exchange transport. Cont Shelf Res 27(1):103–116

Codiga D, Nehra A (2012) Foster-lis gridded data products: Updated methods and appended 2010-2011 observations. Tech. Rep. 2012-01, Graduate School of Oceanography, University of Rhode Island, Narragansett, RI

Deppe W, Thomson J, Polagye B, Krembs C (2018) Predicting deep water intrusions to puget sound, WA (USA), and the seasonal modulation of dissolved oxygen. Estuar Coasts 41(1):114–127

Garrett C, Cummins P (2005) The power potential of tidal currents in channels. Proc R Soc Lond A Math Phys Eng Sci 461(2060):2563–2572

Haas K, Fritz H, French S, Smith B, Neary V (2011) Assessment of energy production potential from tidal streams in the United States. Final Project Report, DE-FG36-08GO18174, Georgia Tech Research Corporation

Lavelle J, Mofjeld H, Lempriere-Doggett E, Cannon G, Pashinski D, Cokelet E, Lytle L (1988) A multiply-connected channel model of tides and tidal currents in Puget Sound, Washington and a comparison with updated observations. Tech. Rep. ERL PMEL-84, NOAA National Ocean Service, Sea and Lake Levels Branch, Rockville, Maryland

Liu Z, Nakamura H, Zhu X, Nishina A, Dong M (2017) Tidal and residual currents across the northern Ryukyu Island chain observed by ferryboat ADCP. J Geophys Res Oceans 122(9):7198–7217

Merckelbach L (2006) A model for high-frequency acoustic Doppler current profiler backscatter from suspended sediment in strong currents. Cont Shelf Res 26(11):1316–1335

Nauw J, Merckelbach L, Ridderinkhof H, Van Aken H (2014) Long-term ferry-based observations of the suspended sediment fluxes through the Marsdiep inlet using acoustic Doppler current profilers. J Sea Res 87:17–29

Palodichuk M, Polagye B, Thomson J (2013) Resource mapping at tidal energy sites. J Ocean Eng 38(3):433–446

Petersen W (2014) FerryBox systems: State-of-the-art in Europe and future development. J Mar Syst 140 Part A(0):4–12

Polagye B, Thomson J (2013) Tidal energy resource characterization: methodolgy and field study in Admiralty Inlet, Puget Sound, USA. Proc Inst Mech Eng Part A J Power Energy 227(3):352–367

Snohomish County Public Utility (2014) Tidal energy research. https://www.snopud.com/PowerSupply/tidal.ashx?p=1155. Accessed Apr 2018

Sutherland D, MacCready P, Banas N, Smedstad L (2011) A model study of the Salish Sea estuarine circulation. J Phys Oceanogr 41(6):1125–1143

Thomson J, Polagye B, Durgesh V, Richmond M (2012) Measurements of turbulence at two tidal energy sites in Puget Sound, WA. IEEE J Ocean Eng 37(3):363–374

Thyng K, Riley J, Thomson J (2013) Inference of turbulence parameters from a ROMS simulation using the k-ε closure scheme. Ocean Model 72:104–118

Yang Z, Khangaonkar T (2010) Multi-scale modeling of Puget Sound using an unstructured-grid coastal ocean model: from tide flats to estuaries and coastal waters. Ocean Dyn 60(6):1621–1637

Zhu XH, Nakamura H, Dong M, Nishina A, Yamashiro T (2017) Tidal currents and Kuroshio transport variations in the Tokara Strait estimated from ferryboat ADCP data. J Geophys Res Oceans 122(3):2120–2142